

Ultrastructural Analysis and TUNEL Demonstrate Motor Neuron Apoptosis in Werdnig-Hoffmann Disease

GORAN SIMIC, MD, PhD, DURDICA SESO-SIMIC, MD, MSc, PAUL J. LUCASSEN, PhD, ATIQUL ISLAM, MD, PhD, ZELJKA KRŠNIK, BBSc, AIDA CVIKO, MD, PhD, DRAZEN JELASIC, MD, PhD, NINA BARISIC, MD, PhD, BENGT WINBLAD, MD, PhD, IVICA KOSTOVIC, MD, PhD, AND BOZO KRUSLIN, MD, PhD

Abstract. Werdnig-Hoffmann disease (WHD) is the most severe clinical type of spinal muscular atrophy characterized by loss of lower motor neurons and paralysis. We examined the hypothesis that disease pathogenesis is based on an inappropriate persistence of normally occurring motor neuron programmed cell death. The diagnosis of WHD was made on the basis of clinical findings, electromyoneurography, and biopsy, and further confirmed by mutation analysis of the survival motor neuron (*SMN*) and neuronal apoptosis inhibitory protein (*NAIP*) genes using PCR. We used ultrastructural analysis as well as TUNEL and ISEL methods to assess DNA fragmentation, and immunocytochemistry to identify expression of the apoptosis-related proteins bcl-2 and p53. A significant number of motor neurons in the spinal cord of children with WHD were shown to die by apoptosis. As revealed by TUNEL, dying neurons in WHD patients comprised 0.2%–6.4% of the neuron numbers counted. This finding contradicts earlier studies that failed to find such evidence and suggests that early blockade of prolonged motor neuron apoptosis may be a potential therapeutic strategy for WHD.

Key Words: Apoptosis; DNA fragmentation; Electron microscopy; Protein p53; Spinal cord; Proto-oncogene proteins c-bcl-2; Werdnig-Hoffmann disease.

INTRODUCTION

The development of the vertebrate nervous system is characterized by an initial overproduction of neurons in many regions followed by large-scale elimination (1). It is estimated that, immediately following the arrival of their axons in muscle cells, about 40%–70% of the embryonic motor neurons in the spinal cord undergo naturally occurring programmed cell death (PCD) during the midgestational period (15–25 weeks of gestation in the human fetus) (1–3).

Werdnig-Hoffmann disease (WHD) is a clinical type I spinal muscular atrophy (SMA type I) and the second most common lethal autosomal recessive disease after cystic fibrosis (4). WHD is characterized by the loss of spinal cord motor neurons, muscular atrophy that starts from birth or from the first months of life onwards, and

progressive paralysis (5). Death usually follows within 2 years of diagnosis.

A gene termed survival motor neuron gene (*SMN*), located at chromosome 5q13, has been identified as the determining gene of SMA because it is deleted in more than 90% of the SMA patients (6). In addition, a neuronal apoptosis inhibitory protein (*NAIP*) gene located near the *SMN* gene has been found to be deleted in 45%–66% of WHD patients, which is considerably more frequently than in any other SMA type (7, 8). Since both the *NAIP* and *SMN* protein exhibit anti-apoptotic activity (9), deletions of the *SMN* and *NAIP* gene may cause apoptosis of motor neurons in the spinal cord in children with WHD (10). However, so far attempts made using the TUNEL method for accessing in situ DNA fragmentation have failed to detect any apoptosis in WHD children (11), or in bovine calves with SMA (12, 13). On the other hand, some apoptotic changes were shown in muscle fibers of children with WHD (14, 15), which has led several authors to propose muscle apoptosis as the main pathogenic mechanism in the disease, which would then result in secondary motor neuron death (16).

The aim of the present study therefore was to re-examine the occurrence of apoptotic cell death in spinal cords of children with clinically, pathologically, and genetically diagnosed and confirmed WHD using TUNEL and electron microscopical analysis. Furthermore, we investigated the in-situ expression of the apoptosis-related proteins bcl-2 and p53 in an immunocytochemical way.

MATERIALS AND METHODS

Clinical Diagnosis and Genotyping

Two groups of children were investigated. The first group consisted of 5 children who died from WHD. The second group

From the Croatian Institute for Brain Research, Department of Neuroanatomy (GS, ZK, IK), Medical School Zagreb, Zagreb, Croatia; University Hospital Rebro, Department of Pediatric Neurology (DS-S, DJ, NB), Medical School Zagreb, Zagreb, Croatia; Division of Medical Pharmacology (P JL), Leiden Amsterdam Centre for Drug Research, Leiden, The Netherlands; Institute for Neurobiology (P JL), Faculty of Biology, University of Amsterdam, Amsterdam, The Netherlands; Karolinska Institute, Department of Clinical Neuroscience and Family Medicine (GS, AI, BW), Huddinge University Hospital, Huddinge, Sweden; and Croatian Institute for Brain Research, Department of Pathology (BK), Medical School Zagreb, Zagreb, Croatia.

Correspondence to: Goran Simic, MD, PhD, Croatian Institute for Brain Research, Zagreb University School of Medicine, Salata 12, 10000 Zagreb, Croatia.

This work was financially supported by the Ministry of Science of the Republic of Croatia (Grant 108-01-01 to IK, grant 108-533 to BK, and grant 108-503 to GS). P JL was supported by the Netherlands Organization for Scientific Research (NWO) and the Internationale Stichting Alzheimer Onderzoek (ISA0).

TABLE
Data from WHD Patients and Controls

WHD patients							First symptoms noticed at (months):	Postmortem time (hours):
Case	Sex	Age	<i>SMN</i> exon 7	<i>SMN</i> exon 8	<i>NAIP</i> exon 5			
1	F	5 months	deleted	normal	deleted		4	4
2	M	5 months	deleted	deleted	deleted		2.5	5.5
3	M	8 months	deleted	normal	deleted		4.5	6
4	M	12 months	deleted	normal	deleted		4	4.5
5	F	22 months	deleted	deleted	normal		5	4

Controls							Postmortem time (hours)
Case	Sex	Age	<i>SMN</i> exon 7	<i>SMN</i> exon 8	<i>NAIP</i> exon 5	Cause of death	
1	F	1 day	normal	normal	normal	congenital heart disease	5
2	F	5 days	normal	normal	normal	congenital heart disease	4.5
3	M	3 months	normal	normal	normal	congenital heart disease	6
4	F	12 months	normal	normal	normal	congenital heart disease	6
5	M	17 months	normal	normal	normal	acute peritonitis	6.5

First symptoms included decreased movements and hypotonia.

consisted of control subjects that did not suffer from any neurological abnormality. The diagnosis was made on the basis of clinical findings, electromyoneurography (EMG) (17), and biopsy, and further confirmed by genetic analysis of blood samples (18). Genotyping was performed using PCR amplifying exons 7 and 8 of the *SMN*, and exon 5 of the *NAIP* gene, which distinguish the *SMN* and *NAIP* telomeric copy from a nonpathogenic gene homologue. Brain tissue was obtained at routine autopsies in accordance with local law and with the permission of the Ethical committee. Informed consent was obtained from all families participating in the study. Patient data from the WHD cases, as well as from the controls, neurologically normal children, are given in the Table.

Histological Procedure and Nissl Staining

Affected muscle tissue fixed in formalin was stained using routine hematoxylin and eosin staining. Following fixation in 4% formaldehyde in PBS (pH 7.4) for several days to weeks, each spinal cord was cut in the rostrocaudal direction in 3-mm-thick slices. To determine shrinkage of the tissue in the period from cutting the slices to final mounting of sections, the areas of 7 randomly chosen slices were determined under a dissecting microscope by using a transparent quadratic grid and reassessed after tissue staining and mounting (19). Following gentle washing in running water, slices were dehydrated through a graded series of ethanol solutions, cleared in toluene, embedded in paraffin (Histowax, Jung) and serially cut in 15- μ m-thick sections. After deparaffinization in xylene, the sections were collected in 70% ethanol, put in 50% and then in 5% ethanol, then put in distilled water, and finally in a staining solution, which consisted of 1 part of 0.5% cresyl-violet in distilled water mixed with 4 parts of distilled water. Upon achieving adequate staining, the sections were placed in distilled water, then passed

through a graded alcohol series and finally in ether-ethanol solution (2 parts of ether and 1 part of 100% ethanol), rinsed with xylene, and mounted.

Electron Microscopy

After fixation in 4% formaldehyde and 1.5% glutaraldehyde in PBS, selected slices of spinal cords were separated under a dissecting microscope in the anterior and posterior halves, and then cut transversely on an ultramicrotome (LKB IV) into semithin sections for light microscopy and stained with toluidine blue. After examination under the light microscope, ultrathin sections were cut on an ultramicrotome (LKB IV) for electron microscopy. The sections were rinsed in 0.1 M Na-cacodylate buffer, postfixed at 4°C for 120 min in 1% OsO₄ in 0.1 M Na-cacodylate buffer, dehydrated in a graded series of ethanol, and embedded in LX112 acetone. The specimens were analyzed in a Philips 420 Electron microscope at 80 kV.

ISEL and TUNEL Immunocytochemistry

ISEL (in-situ end labeling) was performed essentially as described earlier (20, 21). Briefly, sections were deparaffinized in xylene and hydrated to 50% ethanol in distilled water, preincubated with proteinase K (PK) buffer (10 mM Tris/HCl; 2.6 mM CaCl₂; pH 7.0), and incubated with 5 μ g/ml PK (Sigma, Zwijndrecht, The Netherlands) in PK buffer for 15 min at RT. After washing in distilled water, sections were incubated with terminal transferase (TdT) buffer (0.2 M sodiumcacodylate, 0.025 M Tris/HCl in 0.25 mg/ml bovine serum albumin (BSA), pH 6.6) for 15 min at RT and then incubated for 60 min at 37°C with a reaction mixture that contained 0.2 μ l TdT (Boehringer Mannheim, Almere, The Netherlands)/100 μ l reaction mixture and 1.0 μ l biotin-16-dUTP (Boehringer Mannheim)/100 μ l reaction mixture and cobalt chloride (25 mmol/l; 5% of

the final volume). Incorporation of labeled oligonucleotides was ended by rinsing the sections in distilled water and PBS (pH 7.4). Endogenous peroxidase activity was blocked with 0.01% H₂O₂ in PBS for 20 min at RT, after which sections were washed in PBS, preincubated with PBS/1% BSA for 15 min, and incubated with peroxidase-conjugated avidin (ABC-Elite kit, Vector Labs, Burlingame, CA) 1:1000 in PBS/1% BSA overnight at 4°C. Following washing in PBS, labeled DNA was visualized by incubation with 0.5 µg/ml diaminobenzidine (DAB) (Sigma) in 0.05 M Tris/HCl (pH 7.5) with 0.02% H₂O₂ for exactly 12 min. Color development was stopped by washing in distilled water, after which sections were lightly counterstained with methyl-green prior to mounting coverslips. Positive controls consisting of sections from rat prostate 3 days after castration were included in every assay (21). All sections from control and WHD patients were labeled after random selection under identical experimental conditions. TUNEL (terminal deoxynucleotidyl-transferase (TdT)-mediated dUTP-biotin nick end labeling) method was implemented using the in situ cell death detection kit (Boehringer Mannheim, cat. no. 1684817), as described before (22). In short, sections were incubated with sheep anti-fluorescein antibody conjugated with horseradish peroxidase. Incorporated, labeled DNA was visualized using DAB with a metal enhanced substrate as described by the manufacturer (cat. no. 1718096, Boehringer Mannheim). In negative controls, TdT was omitted, while positive controls included DNase I (1 mg/ml for 10 min at RT) treatment to induce DNA strand breaks.

Quantitative Analysis of Neuron Numbers

Estimates of the reference volume were made by delineation of the anterior horns with a drawing microscope Nikon Alaphot2-YS2-H and using Cavalieri's principle. Numerical density of the neurons was obtained using a modification of the physical dissector method suited for use with a drawing microscope (23). The total number of neurons was obtained by multiplying the numerical density with the reference volume of the measured anterior horn and included a correction for 3-dimensional tissue shrinkage. Assuming that shrinkage is similar for all 3 dimensions, shrinkage in the third dimension was assessed by calculating the square root of the measured areal shrinkage as a correction factor for the factor "slice thickness" in the formula of Cavalieri. The difference in neuron numbers between the WHD and the control group was evaluated with the Student *t* test, while the difference in proportions of TUNEL-positive versus the total number of unaffected neurons was assessed using the Chi-square test.

Bcl-2 and p53 Immunocytochemistry

Monoclonal antibodies were obtained from DAKO, Glostrup, Denmark (bcl-2 cat. no. M0887, p53 cat. no. M7001). Immunocytochemistry was performed using the ABC Elite kit (Vector Labs). The sections were incubated in primary antibody solution in a dilution of 1:80 (bcl-2) or 1:40 (p53) for 120 min at 37°C. Positive controls were included and consisted of a section taken from normal breast (for bcl-2) and breast carcinoma (for p53).

RESULTS

Hematoxylin and eosin staining revealed typical neurogenic muscle atrophy in all WHD patients that was absent in the controls. In Nissl stained sections of WHD patients, but not in controls, marked neuron loss of the anterior horns was obvious at all levels of the spinal cord investigated (Fig. 1A, B). Besides neurons that appeared normal and healthy, many of the remaining anterior horn neurons in the WHD tissue were ballooned (ballooned neurons, BNs). At the light microscopical level, BNs displayed several morphological changes ranging from swelling, chromatolysis, and peripheral displacement of the nucleus (Fig. 1C–E) to microvacuolation and disintegration of the nuclear and cytoplasmic membrane (Fig. 1F–H). In addition, groups of microglial cells were often found to be accumulated around, and in close association with BNs (Fig. 1I). Among the apparently normal as well as among BNs in the WHD tissue, smaller numbers of neurons with nuclear and cytoplasmic condensation, clumping of chromatin, and loss of Nissl granules were observed (Fig. 1J). These hallmarks suggested that they were apoptotic. Furthermore, along the anterior spinal nerve roots in children with WHD, heterotopic (migratory) motor neurons and bundles of astroglial cells were found.

Electron microscopical analysis in the tissue from children with WHD revealed neurons with a clearly apoptotic ultrastructural morphology (type 1 according to classification of Clarke) that could not be found in controls (24, 25) (Fig. 2A–D). The apoptotic changes varied from moderate condensation of both nucleus and cytoplasm, and nuclear membrane hyperchromatosis (Fig. 2A–C), to a pronounced reduction and reshaping of both nucleus and cytoplasm, a loss of ribosomes from the rough ER and polysomes, and the presence of apoptotic bodies (Fig. 2D, E). Occasionally, degenerating neurons with a combination of type 1 (apoptosis) and type 2 cell death (autophagic degeneration) were found as well (Fig. 2E). Changes in the BNs in WHD patients ranged from moderate swelling and peripheral displacement of the nucleus and rough ER, to an extensive swelling in association with a more round shape of the cell, 'vacuolization' of the cytoplasmic organelles (Fig. 2F) and a loss of structure accompanied by breakdown of the plasma membrane. Together, these ultrastructural criteria indicated the presence of necrotic cell death (25).

In contrast to controls, who were virtually free of any TUNEL or ISEL-positive cells (Fig. 3A), in all children with WHD both TUNEL (Fig. 3B, C) and ISEL (Fig. 3D, E) revealed a substantial number of anterior horn motor neurons, as well as glial cells, that displayed fragmented DNA. Most of the TUNEL/ISEL-positive neurons showed morphological features of apoptosis: condensation of the nucleus and cytoplasm, margination of

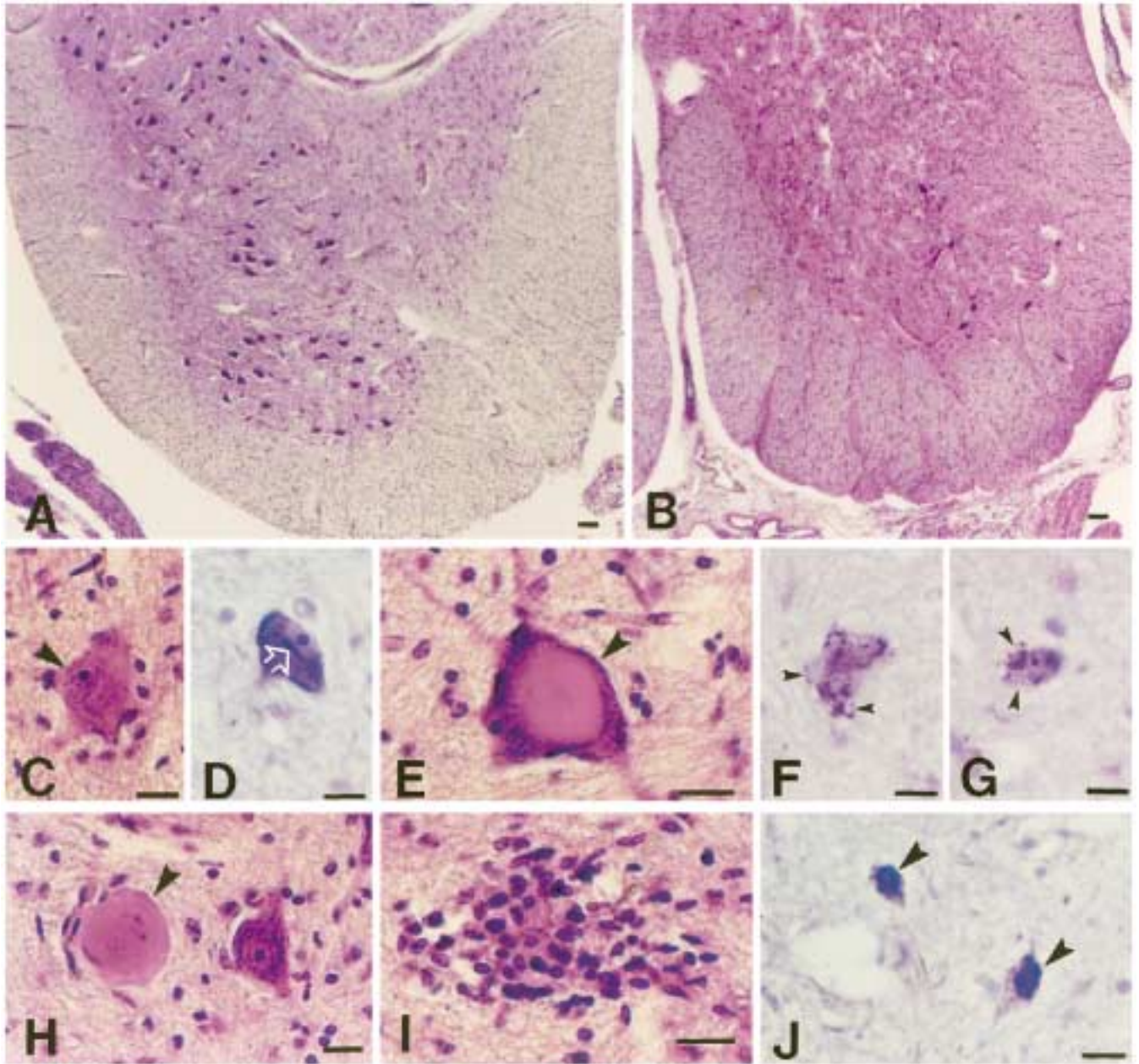


Fig. 1. Motor neuron changes in the anterior horn in WHD as revealed by Nissl stain. A: Normal control at the same level as (B). B: Marked loss of the anterior horn neurons at the midthoracic level of the spinal cord of a child with WHD. C–E: Ballooned neurons (BNs) in an early stage of degeneration. Morphological changes include the nucleus displaced towards periphery of cytoplasm (C, arrowhead), occasionally with a mass of Nissl granules arranged as a ‘nuclear cap’ (D, arrow), prominent nucleolus, swelling of perikaryon and central chromatolysis of the Nissl granules (E, arrowhead). F–H: BNs in an advanced stage of degeneration showing cytoplasmic vacuolization (F, arrows) and hypochromasia. Disintegration of cytoplasmic membrane leads to spilling of BNs’ contents into surrounding neuropil (G, arrows), while BNs without disrupted cytoplasmic membrane show rounding up of the cell and appear uniformly structureless and achromatic (H, arrowhead). I: Neuronophagia of BNs by microglial cells. J: Two apoptotic-like motor neurons with nuclear and cytoplasmic condensation, clumping of chromatin (arrowheads) and loss of Nissl granules. Scale bars: A and B, 100 μ m; C–I, 10 μ m; J, 5 μ m.

condensed chromatin, blebbing of both the nucleus and plasma membrane, and segregation and disintegration of the nucleus. Neurons with fragmented DNA were frequently observed in close association with ISEL-positive glial cells (Fig. 3D, E). ISEL and TUNEL staining

labeled the glial cells that resembled microglia cells throughout their cytoplasm and protrusions, but often with an intact, unstained nucleus (Fig. 3D, E). However, (micro)glial cells with fragmented DNA in their nucleus were also observed, particularly when these

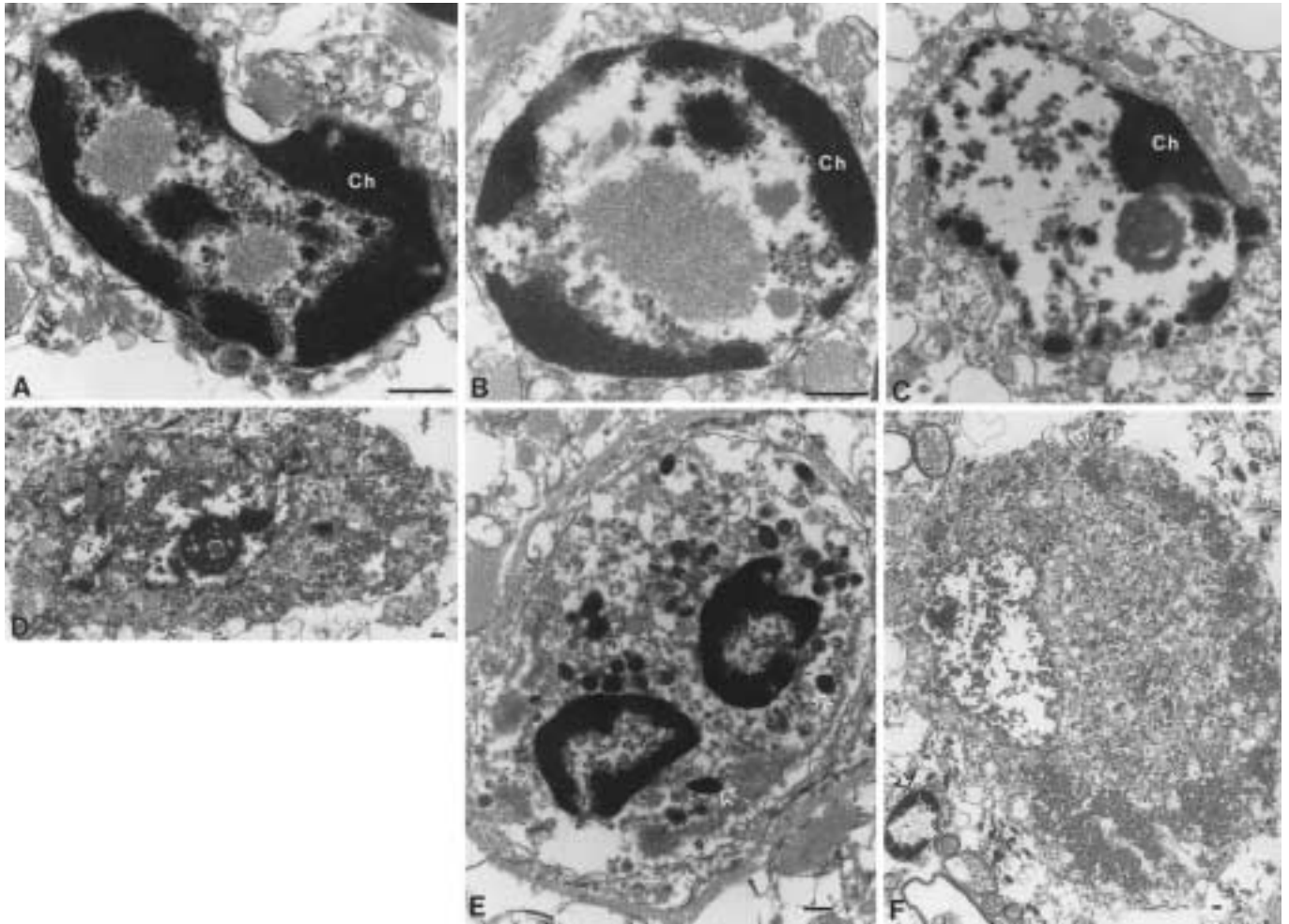


Fig. 2. Electron microscopic appearance of anterior horn neurons in children with WHD. A–C: Nuclei of motor neurons in the early to middle stage of apoptotic degeneration. Considerable condensation of nuclei is seen together with chromatin masses (Ch) accumulated mainly at the nuclear rim. D: Motor neuron in the late stage of apoptotic degeneration. Pronounced reduction and reshaping of both nucleus and cytoplasm, loss of ribosomes from the rough ER and polysomes, and segregation into apoptotic bodies are seen. E: A motor neuron showing features of both apoptosis (hyperchromatosis of nuclear membrane, segregation of the nucleus into apoptotic bodies) and autophagic degeneration (autophagic vacuoles, arrows). F: A swollen and rounded ballooned neuron (BN) showing peripheralization of nucleus and Nissl granules by central accumulation of mitochondria, vesicles, and dispersed Nissl granules among which are scattered neurofilaments. In the lower left corner an apoptotic microglial cell is seen as judged from its small size and clumping of the chromatin along the inner side of the nuclear envelope (arrow). Scale bars: 1 μ m.

cells seemed to participate in the neuronophagia of BNs (Figs. 2F, 3E). In WHD cases, TUNEL/ISEL-positive cells were also found in the nucleus thoracicus (Clarke's column or Rexed's lamina VII), while BNs in the anterior horn were never TUNEL/ISEL-positive (Fig. 3F).

Two-dimensional (areal) shrinkage of the Nissl stained tissue was on average 21.0% (minimum 10.5%, maximum 32.7%, SD 8.5%) in the WHD group, and 13.9% (minimum 4.8%, maximum 22.9%, SD 6.2%) in the control group. Quantitative analysis of neuron number in these sections showed that compared with controls, on average, 73% of the neurons were lost in WHD ($t = 19.9$, d.f. = 8, $p \ll 0.01$) (Fig. 4). As revealed by TUNEL, dying neurons in WHD patients comprised 0.2%–6.4%

of the neuron numbers counted. The proportion of TUNEL-positive neurons versus the total number of neurons left over was greater in children who died at a younger age (chi-square = 9.5, d.f. = 4, $p < 0.05$) (Fig. 4). TUNEL-positive glial cells that were not counted outnumbered the TUNEL-positive neurons.

Bcl-2 immunocytochemistry revealed a pronounced loss of cytoplasmic expression in remaining motor neurons as well as in glial cells of all WHD cases, while the control subjects showed only moderate to strong bcl-2 immunopositivity (Fig. 5A, B). Motor neuron nuclear expression of p53 protein was very strong in all WHD cases while it was variable, but always much weaker in controls (Fig. 5C, D).

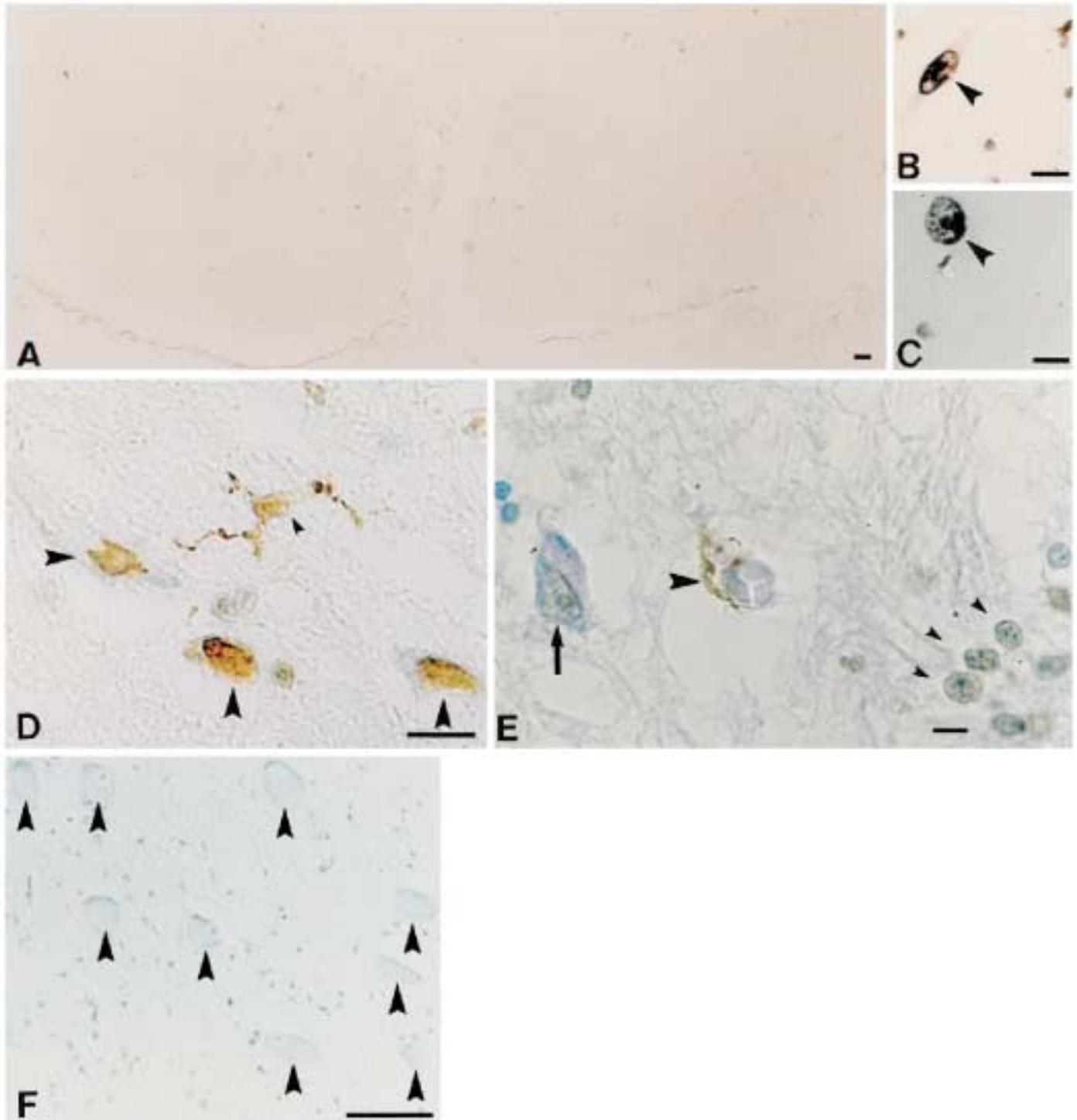


Fig. 3. TUNEL (A, B and C) and ISEL (D and E) staining of the anterior horns in 1 control subject (A) and in children with WHD (B–E). ISEL is counterstained with methyl-green. A: Control spinal cord virtually free of any TUNEL immunoreactivity. Dark spots represent artifactual staining. B and C: Two examples of TUNEL-positive motor neurons found (arrowheads). D: Apoptotic motor neurons (arrowheads) showing pronounced condensation and ISEL-positive nuclei. Small arrowhead shows ISEL-positive glial cell. E: An apoptotic motor neuron (note pronounced condensation and segregation of the neuron) engulfed by an ISEL-positive glial cell (large arrowhead). At the bottom right corner ISEL-positive nuclei of microglial cells are seen that appear to be involved in neuronophagia of BNs (small arrowheads). Arrow shows weakly ISEL-positive neuron probably representing an early stage of the apoptotic process. F: ISEL-negative BNs (arrowheads). Scale bars: A and F, 100 μm ; B–E, 10 μm .

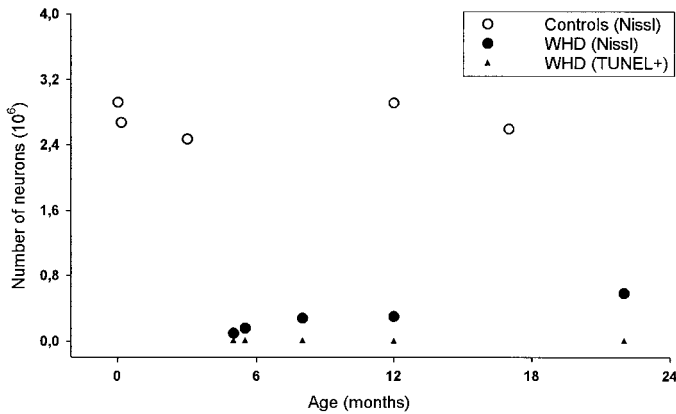


Fig. 4. Total number of anterior horn neurons as quantified on Nissl and TUNEL-stained sections using the Cavalieri principle and the physical disector method. The open circles represent controls and the black circles WHD cases. The black triangles represent the estimated numbers of TUNEL-positive apoptotic neurons.

DISCUSSION

Our results clearly demonstrate that a significant number of motor neurons in the spinal cord of children with WHD, but not in controls, die by a process that has all the morphological characteristics of apoptosis (cell death type 1 according to Clarke) (24, 25), including condensation of chromosomal DNA, membrane blebbing, apoptotic bodies, and reduction in cell and nuclear volume.

The characteristic morphological profile of apoptotic cells at the electron microscopic level was further accompanied by detection of the extensive fragmentation of the chromatin as identified by TUNEL and ISEL, together with morphological hallmarks. Compared with controls, that are free of TUNEL/ISEL positivity, strong and extensive labeling was found in motor neuron nuclei in WHD cases. As TUNEL/ISEL in fact recognizes DNA damage that is associated with both apoptosis and necrosis, only the additional presence of convincing apoptotic morphology allows us to convincingly identify apoptotic from necrotic cell death (25). Although many TUNEL/ISEL-positive neurons in our WHD tissue show morphological characteristics of apoptosis, some neurons containing fragmented DNA do not fulfill the morphological criteria for apoptosis and rather appear necrotic. Recent studies indicate that these types of cell death may also overlap (25, 26), which may, to some extent, be involved in the present disorder as well. For instance, fast initial induction of apoptosis in WHD could be followed by slower secondary necrosis, which would explain why not all TUNEL/ISEL-positive cells show apoptotic features. Nevertheless, by studying these cells at the ultrastructural level, we have convincingly identified true apoptosis with all stages of typical apoptotic cell death present, ranging

from initial accumulation of chromatin masses in the nucleus, to pronounced condensation of both nucleus and cytoplasm, and segregation into apoptotic bodies.

The apoptotic mechanism of cell death is further supported by the prominent phagocytosis of fragmented DNA by microglial cells that were also TUNEL-positive. TUNEL/ISEL labeling of microglia cells throughout their cytoplasm including the protrusions, but often with an intact nucleus, suggests that these cells have indeed phagocytosed dying apoptotic neurons rather than that they are undergoing apoptosis themselves. Microglia with positive nuclear TUNEL/ISEL labeling were also sometimes observed, but then only when these cells participated in neuronophagia of BNs. In this case, apoptosis is perhaps just a physiological mechanism by which excess amounts of microglial cells are eliminated.

Several possible reasons may account for the lack of success in previous attempts to detect apoptosis in WHD by using only TUNEL (11–13). One of them could be the masking effect due to overfixation, which is known to hamper ISEL outcome seriously (20, 27). Furthermore, an inadequate sample size of sections analyzed and the absence of genotyping needed for the identification of actual mutations in the *SMN* and *NAIP* gene may have been involved in these previous studies as well.

Examination of the remaining anterior horn neurons in children with WHD revealed that many of them were ballooned (BNs) and displayed chromatolysis as well as other changes characteristic for retrograde axonal degeneration. However, although BNs in WHD share many morphological features with chromatolytic neurons following axotomy, a differential distribution of phosphorylated neurofilaments and ubiquitin within the perikarya of BNs suggest that BNs should not be viewed as a form of chromatolytic neuronal death secondary to axonal injury (28). Rather, BNs in WHD may reflect another pathogenic mechanism of neuronal injury that involves the metabolism of neurofilaments, which most probably relates to dissociated phosphorylation and glycosylation (29). According to this view, aberrant glycosylation also causes a defect in the assembly of neuron-glia adhesion molecules that may affect or induce migratory motor neurons and glial bundles around spinal roots, which have been observed in this study as well. The continuum of morphological changes observed in the BNs in the present WHD patients at both the light and electron microscopic level thus seems to correspond to the necrotic type of cell death (25).

The number of apoptotic neurons found in anterior horns of the spinal cord of WHD patients studied is relatively low (0.2%–6.4% of the remaining motor neurons). This finding is in line with the expected and estimated rapid process of apoptosis in brain tissue (30–35). As apoptosis in fact represents a turnover state rather than a fixed entity (e.g. cell number), the chance of detecting

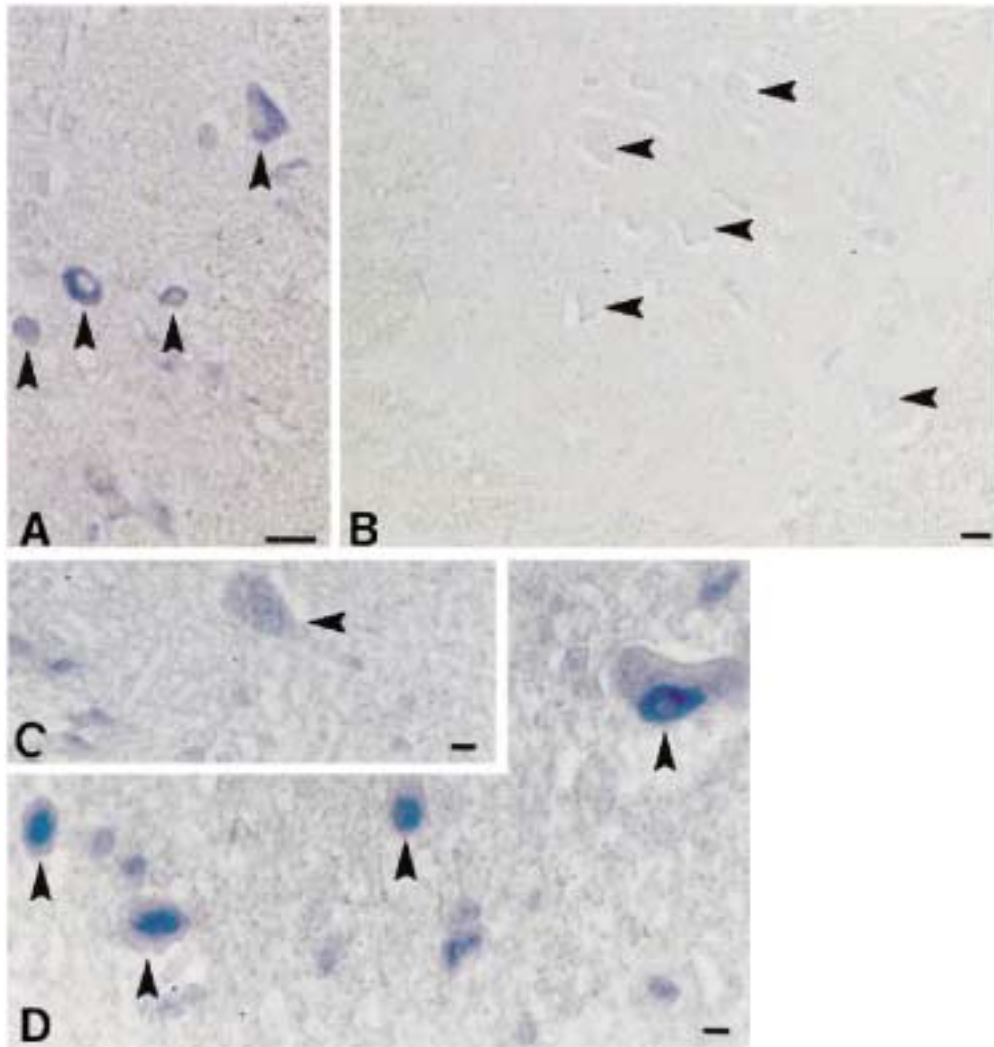


Fig. 5. A: Moderate to strong *bcl-2* immunopositivity in control spinal cord (arrowheads). B: Loss of cytoplasmic expression of *bcl-2* protein in a WHD patient (arrowheads show *bcl-2*-negative neurons). C: Weak p53 staining in control spinal cord (arrowhead). D: Strong motor neuron nuclear expression of p53 protein in a WHD patient (arrowheads). Scale bars: A and B, 50 μm ; C and D, 10 μm .

it in thin tissue sections at a given time point is low. Therefore, the cumulative total amount of neurons dying through apoptosis in WHD is most probably strongly underestimated. This conclusion is supported by the fact that, on average, only about 27% of normal motor neuron numbers are left in patients with WHD, which implies that most of the missing neurons may have died by apoptosis before. Also, the relative proportion of TUNEL-positive/Nissl neurons is greater in children with more severe forms of the disease (i.e. in those who died at younger ages). This also suggests that apoptosis may be more extensive in earlier phases of the disease. Since it has been reported that immature neurons may be prone to die by apoptosis, whereas later in development they may be more likely to die by the slower necrosis-like type of death (25), age of the motor neurons may possibly influence the type of cell death as well.

Bcl-2-related proteins form an important class of apoptosis-regulatory gene product (36). Expression of the apoptosis-inhibitory *bcl-2* gene under the control of tissue specific promoters has been shown to protect many different cell types against apoptosis, particularly motor neurons of the spinal cord (37). The current *bcl-2* immunocytochemistry in human neurons revealing an apparent loss of cytoplasmic expression in patients with WHD favors a scenario in which apoptotic cell death contributes to motor neuron degeneration in WHD.

The apoptosis-inducing p53 protein regulates the death of neurons both after DNA damage and during development (38). Nuclear positivity for p53, as currently found in WHD patients, indicates the presence of a p53-mediated apoptotic pathway in motor neurons in the WHD tissue. Large-scale deletions of the 5q13 region specific to WHD (7) may be an additional factor

for induction and strong p53 expression in motor neurons during the disease.

In conclusion, this is the first report to show convincing apoptotic cell death in anterior horn cells of the spinal cord in children with WHD. This is clear not only from TUNEL- and ISEL-positive motor neurons but also from ultrastructurally confirmed apoptotic morphology, which was generally absent in controls. This suggests that at least part of the neuronal death in WHD occurs by apoptosis. Moreover, with the known time kinetics of apoptosis in mind, its present identification implies that an active process of apoptosis may even have played a primary role in the neuron loss in earlier stages of the disease. The occurrence of apoptosis as a possibly predominant mechanism of neuronal death in WHD may be important with respect to future strategies directed towards a cytoprotective therapy of WHD.

ACKNOWLEDGMENTS

Thanks to Dr. J. Sertic (University Hospital Rebro, Zagreb), Dr. M. Heffer-Lauc, Z. Cmuk, D. Budinscak, B. Popovic (Croatian Institute for Brain Research, Zagreb), and I. Jusinsky (Clinical Research Center—Electron microscopy unit, Huddinge University Hospital, Karolinska Institute, Stockholm) for excellent technical assistance.

REFERENCES

- Clarke PGH. Neuronal death in the development of the vertebrate central nervous system. *Sem Neurosci* 1994;6:291–97
- Oppenheim RW. Cell death during development of the nervous system. *Annu Rev Neurosci* 1991;14:453–501
- Yachnis AT, Giovanni MA, Eskin TA, Reier PJ, Anderson DK. Developmental patterns of bcl-2 and bcl-x polypeptide expression in the human spinal cord. *Exp Neurol* 1998;150:82–97
- Gomez MR. Motor neuron diseases in children. In: Engel AG, Franzini-Armstrong C, eds. *Myology*. New York: McGraw-Hill, 1994:1837–57
- Dubowitz V. Disorders of the lower motor neuron, the spinal muscular atrophy. In: Dubowitz V, ed. *Muscle disorders in childhood*, 2nd ed. London: Saunders, 1995:325–69
- Lefebvre S, Burglen L, Reboullet S, et al. Identification and characterization of a spinal muscular atrophy-determining gene. *Cell* 1995;80:155–65
- Burlet P, Burglen L, Clermont O, et al. Large scale deletions of the 5q13 region are specific to Werdnig-Hoffmann disease. *J Med Genet* 1996;33:281–83
- Roy N, Mahadevan MS, McLean M, et al. The gene for neuronal apoptosis inhibitory protein is partially deleted in individuals with spinal muscular atrophy. *Cell* 1995;80:167–78
- Iwahashi H, Eguchi Y, Yasuhara N, Hanafusa T, Matsuzawa Y, Tsujimoto Y. Synergistic anti-apoptotic activity between Bcl-2 and SMN implicated in spinal muscular atrophy. *Nature* 1997;390:413–17
- Morrison KE. Advances in SMA research: Review of gene deletions. *Neuromusc Disord* 1996;6:397–408
- Hayashi M, Arai N, Murakami T, Yoshio M, Oda M, Matsuyama H. A study of cell death in Werdnig-Hoffmann disease brain. *Neurosci Lett* 1998;243:117–20
- Ferrer I. Motoneuron diseases: A type of programmed cell death? *Neurologia* 1996;11(Suppl 5):7–13
- Pumarola M, Anor S, Majo N, Borrás D, Ferrer I. Spinal muscular atrophy in Holstein-Friesian calves. *Acta Neuropathol* 1997;93:178–83
- Tews DS, Goebel HH. DNA fragmentation and bcl-2 expression in infantile spinal muscular atrophy. *Neuromusc Disord* 1996;6:265–73
- Tews DS, Goebel HH. Apoptosis-related proteins in skeletal muscle fibers of spinal muscular atrophy. *J Neuropathol Exp Neurol* 1997;56:150–56
- Fizdianska A, Goebel HH, Warlo I. Acute infantile spinal muscular atrophy. Muscle apoptosis as a proposed pathogenetic mechanism. *Brain* 1990;113:433–45
- Barisic N, Sertic J, Billi C, et al. Molecular analysis and electromyographic abnormalities in Croatian children with proximal spinal muscular atrophies. *Clin Chem Lab Med* 1998;36:667–69
- Sertic J, Barisic N, Sostarko M, et al. Deletions in the *SMN* and *NAIP* genes in patients with spinal muscular atrophy in Croatia. *Coll Antropol* 1997;21:487–92
- Uylings HBM, Van Eden CG, Hofman MA. Morphometry of size/volume variables and comparison of their bivariate relations in the nervous system under different conditions. *J Neurosci Methods* 1986;18:19–37
- Lucassen PJ, Chung WCJ, Vermeulen JP, Van Lookeren Campagne M, Van Dierendonck JH, Swaab DF. Microwave-enhanced in situ end-labeling of fragmented DNA: Parametric studies in relation to post mortem delay and fixation of rat and human brain. *J Histochem Cytochem* 1995;43:1163–71
- Wijsman JH, Jonker RR, Keijzer R, Van de Velde CJH, Cornelisse CJ, Van Dierendonck JH. A new method to detect apoptosis in paraffin sections: In situ end labeling of fragmented DNA. *J Histochem Cytochem* 1993;41:7–12
- Gavrieli Y, Sherman Y, Ben-Sasson SA. Identification of programmed cell death in situ via specific labeling of nuclear DNA fragmentation. *J Cell Biol* 1992;119:493–501
- Gunthinas-Lichius O, Mockenhaupt J, Stennert E, Neiss WF. Simplified nerve cell counting in the rat brainstem with the physical disector using a drawing microscope. *J Microsc* 1993;172:177–80
- Clarke PGH. Developmental cell death: Morphological diversity and multiple mechanisms. *Anat Embryol* 1990;181:195–213
- Clarke PGH. Apoptosis versus necrosis: How valid a dichotomy for neurons? In: Koliatsos VE, Ratan RR, eds. *Cell death and diseases of the nervous system*. Totowa, New Jersey: Humana Press, 1999:3–28
- Portera-Cailliau C, Price DL, Martin LJ. Excitotoxic neuronal death in the immature brain is an apoptosis-necrosis morphological continuum. *J Comp Neurol* 1997;378:70–87
- Lucassen PJ, Negoesar A, Labat-Moleur F, Van Lookeren Campagne M. Microwave-enhanced in situ end labeling of apoptosis in tissue sections: Pitfalls and possibilities. *Biotechniques* 2000 (in press)
- Murayama S, Bouldin TW, Suzuki K. Immunocytochemical and ultrastructural studies of Werdnig-Hoffmann disease. *Acta Neuropathol* 1991;81:408–17
- Chou SM, Wang HS. Aberrant glycosylation/phosphorylation in chromatolytic motoneurons of Werdnig-Hoffmann disease. *J Neurol Sci* 1997;152:198–209
- Majno G, Joris I. Apoptosis, oncosis and necrosis: An overview of cell death. *Am J Pathol* 1995;146:3–15
- Perry G, Nunomura A, Smith MA. A suicide note from Alzheimer disease neurons? *Nature Med* 1998;4:897–98
- Conti AC, Raghupathi R, Trojanowski JQ, McIntosh TK. Experimental brain injury induces regionally distinct apoptosis during the acute and delayed post-traumatic period. *J Neurosci* 1998;18:5663–72
- Lucassen PJ, Chung WCJ, Kamphorst W, Swaab DF. DNA damage distribution in the human brain as shown by in situ end labeling: Area-specific differences in aging and Alzheimer disease in the absence of apoptotic morphology. *J Neuropathol Exp Neurol* 1997;56:887–900
- Perry G, Nunomura A, Lucassen PJ, Lassmann H, Smith MA. Apoptosis and Alzheimer's disease. *Science* 1998;282:1268–69

35. Stadelman C, Bruck W, Bancher C, Jellinger K, Lassmann H. Alzheimer's disease—DNA fragmentation indicates increased neuronal vulnerability, but not apoptosis. *J Neuropathol Exp Neurol* 1998;57:456–64
36. Kroemer G. The proto-oncogene *bcl-2* and its role in regulating apoptosis. *Nature Med* 1997;3:614–20
37. Martinou JC, Dubois-Dauphin M, Staple JK, et al. Overexpression of *bcl-2* in transgenic mice protects neurons from naturally occurring cell death and experimental ischaemia. *Neuron* 1994;13:1017–30
38. Cregan SP, MacLaurin JG, Craig CG, et al. Bax-dependent caspase-3 activation is a key determinant in p53-induced apoptosis in neurons. *J Neurosci* 1999;19:7860–69

Received November 24, 1999

Revision received February 4, 2000

Accepted February 7, 2000